

Crystalline Structure and Morphology of Poly(L-lactide) Formed Under High Pressure

Chaosheng Yuan, Xuerui Cheng, Xiang Zhu, Yongqiang Wang, Kun Yang, Zheng Wang, Lei Su

The High Pressure Research Center of Science and Technology, Department of Physics and Electronic Engineering, Zhengzhou University of Light Industry, Zhengzhou 450002, China
Correspondence to: C. Yuan (E-mail: zzyuancs@163.com)

ABSTRACT: The poly(L-lactide) (PLLA) samples were prepared by the annealing under 100 MPa at 75–145°C and 200 MPa at 105–145°C for 6 h, respectively. The crystalline structures, thermal properties and morphology were investigated using differential scanning calorimetry (DSC), wide-angle X-ray diffraction (WAXD), and scanning electron microscopy (SEM). On the basis of the DSC and WAXD results, it can be seen that the α' form was formed by the annealing under 100 MPa at 85–95°C but not found under 200 MPa at 105–145°C. A phase diagram of PLLA crystal form under high pressure was constructed under the given experimental conditions, which displayed the α' form was formed at limited temperature and pressure range. Besides, SEM suggested that the PLLA samples annealed under 100 MPa crystallize to form lamellar-like crystals due to the low growth rate and the confined crystallization behavior under high pressure. © 2014 Wiley Periodicals, Inc. *J. Appl. Polym. Sci.* **2014**, *131*, 40637.

KEYWORDS: biopolymers and renewable polymers; crystallization; morphology; phase behavior

Received 19 December 2013; accepted 23 February 2014

DOI: 10.1002/app.40637

INTRODUCTION

Poly(L-lactide) (PLLA) as a biodegradable polymer, has attracted considerable interest from both fundamental and practical perspectives because it is producible from renewable sources, and is thus environmentally and economically appropriate.^{1–3} Since it degrades to nontoxic lactic acid, which is naturally present in the human body, poly(lactic acid) can be used in biomedical fields, such as implant materials, surgical suture, and controlled drug delivery systems.^{4,5} Furthermore, the attribute of biodegradability, producibility from renewable products, and good mechanical properties makes it a promising material for many disposable products, such as baby diapers, cups, plastic bags, and films.

Depending on the crystallization condition, PLLA forms several types of crystalline modification, the α ,⁶ β ,⁷ and γ ⁸ forms. Furthermore, another crystalline modification, the α' (disorder α) form, was studied by many researchers recently.^{9–13} The α' crystals are formed by the crystallization below 100°C, while the α ones are developed by the crystallization above 120°C.^{9,11,12} And the α' -form is considered as a conformationally disordered α -crystal with slightly increased lattice spacings and transforms upon heating into the stable α form.¹⁴ Nevertheless, there are few publications relevant to the high pressure behavior of PLLA. Ahmed et al. reported that the degree of crystallinity of

PLLA remarkable decreases when the treated pressure increases to about 650 MPa.¹⁵ Asai et al. revealed that the crystal modification changes continuously from the disorder α to α forms not through the α' one with increasing temperature under high-pressure CO₂.¹⁶ Huang et al. reported that the α' is formed under pressure of 100 MPa and above, and α' crystal structure transformed to α one is observed by time-resolved synchrotron SAXS.¹⁷ In fact, investigation on the high pressure behavior of PLLA has important significance regardless of its microstructure or understanding of the potential application.

In this article, we report the crystallization behavior and morphology of PLLA by annealing under high pressure. The crystalline structure, melting behavior and morphology are investigated employing differential scanning calorimetry (DSC), wide-angle X-ray diffraction (WAXD), and scanning Electron Microscope (SEM) methods, respectively. Furthermore, the phase diagram of PLLA crystal form under pressures up to 200 MPa is constructed from the DSC and WAXD results.

EXPERIMENTAL

Materials

In this study, PLLA was purchased from Sigma-Aldrich. The average molecular weight (M_w) of 67,000 and a polydispersity index (M_w/M_n) of 1.4 was determined by gel permeation chromatograph (GPC).

Table I. The Annealed Conditions and the Thermodynamic Parameters Obtained from DSC Measurements

Sample	Annealing temperature T_a (°C)	Annealing pressure P_a (MPa)	Melting point T_m (°C)		Crystallization enthalpy ΔH_c (J/g)	Melting enthalpy ΔH_m (J/g)	Crystallinity X_c (%)
			T_{m-low}	T_{m-high}			
PLLA-amorphous	-	-	168.8	175.3	41.9	66.6	16
PLLA-0.1-130	130	0.1	163.2	175.3	-	63.8	45
PLLA-100-75	75	100	169.6	176.2	38.17	64.7	18
PLLA-100-85	85	100	171.6	174.5	7.014	66.2	41
PLLA-100-95	95	100	171.5	175.5	-	65.9	46
PLLA-100-105	105	100	173.4	175.7	-	67.6	47
PLLA-100-115	115	100	171.9	176.7	-	71.4	50
PLLA-100-130	130	100	162.6	169.6	-	82.1	58
PLLA-100-145	145	100	162.0	164.4	-	73.4	52
PLLA-200-105	105	200	167.8	177.5	42.70	68.8	18
PLLA-200-110	110	200	169.1	174.4	36.91	64.6	19
PLLA-200-115	115	200	171.1	174.9	-	65.4	46
PLLA-200-130	130	200	163.2	167.3	-	78.9	56
PLLA-200-145	145	200	162.3	166.9	-	76.0	53

The samples were named as PLLA- P_a - T_a .

Sample Preparation and High Pressure Equipment

To prepare samples annealed at different temperature and high pressure conditions, the PLLA pellets were quickly quenched in ice water after melting at 200°C for 1 min to obtain the amorphous samples first. The resultant film was dried under vacuum at room temperature for ca. 1 day to remove water. High-pressure experiments were carried out by using high-pressure apparatus. A set of piston-cylinder made of tungsten carbide with a resistance coil heater was used to produce high pressure and temperature. The diameter of the cylinder was 20 mm. Each of the obtained amorphous PLLA was filled in an aluminum container with an inner diameter of 18 mm and depth of 1 mm. The details of the sample assembly and the pressure and temperature calibrations were the same as those described in previous article.¹⁸ After loading the amorphous sample, the pressure was raised to the predetermined level, and then the temperature was raised to the predetermined level. The samples were annealed under the constant temperature-pressure conditions for 6 h, and then cooled naturally by turning off the power to room temperature and finally decompressed slowly. As a comparative investigation, another PLLA sample was prepared under ambient pressure (around 0.1 MPa) by annealing at 130°C for 6 h. These annealing conditions are listed in Table I.

Differential Scanning Calorimetry

DSC measurements were carried out using a TA Q-100 instrument at a heating rate of 10°C/min in the temperature range from 25 to 190°C under a nitrogen gas atmosphere. The degree of crystallinity x_{c_DSC} for each PLLA sample was calculated from the following equation:

$$x_{c_DSC} = \frac{\Delta H_m - \Delta H_c}{\Delta H_m^0} \times 100$$

where ΔH_m^0 is the heat of fusion for the perfectly crystalline PLLA, which was assumed to be 142 J/g according to

Hoffman,¹⁹ ΔH_m is the heat of fusion for PLLA during a DSC heating run, and ΔH_c is the heat of crystallization for PLLA during a DSC heating run.

Wide-Angle X-ray Diffraction Measurement

WAXD investigations of the samples annealed at different conditions were performed using a Bruker Nanostar System, with incident X-ray radiation source which is Ni-filtered Cu K α radiation at a wavelength $\lambda = 0.1542$ nm. All the measurements were operated at 30 kV and 20 mA from 10° to 35° at a 2θ scan rate of 3°/min.

Scanning Electron Microscope

SEM investigations were performed using a Hitachi S3400+EDX SEM instrument with an acceleration voltage of 10 kV to examine the microscopic morphology of the impact fractured surfaces of the specimens. They were cryo-fractured in liquid nitrogen and coated with a thin layer of gold to improve their conductivity prior to SEM observation.

RESULTS AND DISCUSSION

DSC Measurements

Figure 1 show the DSC curves of the PLLA samples annealed under ambient pressure, 100 MPa, and 200 MPa, different temperatures for 6 h, and the melting temperature (T_m), melting enthalpy (ΔH_m) and crystallinity (x_{c_DSC}) for different samples are listed in Table I. To compare easily, the DSC results of initial amorphous PLLA is also shown here. It is confirmed that no crystallization occurs after the sample is annealed under 100 MPa at 75°C for 6 h, because the DSC curve of the corresponding sample shows the obvious exothermic and endothermic behavior, which corresponds to the glass transition, crystallization and melting of PLLA during the thermal scan. The similar results are also observed for the initial amorphous sample.

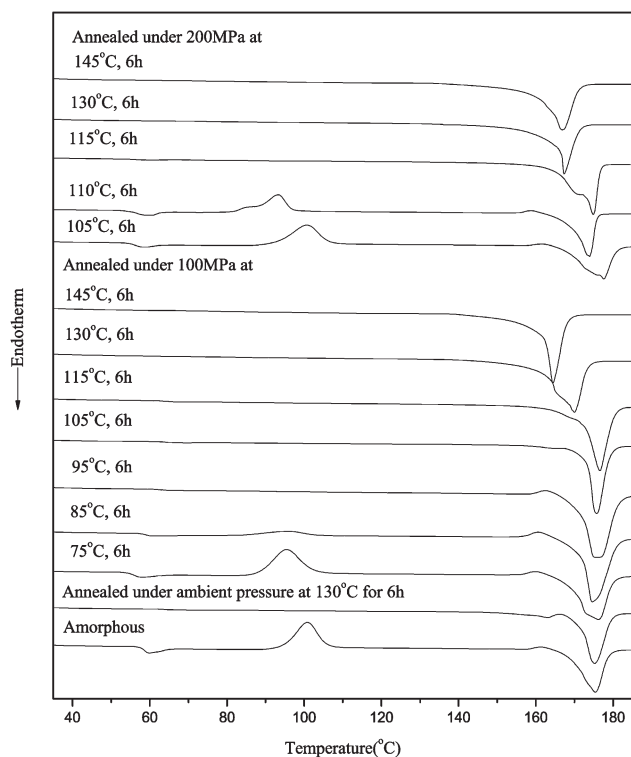


Figure 1. DSC curves of the PLLA films annealed under different pressure–temperature conditions and initial amorphous one.

However, the crystallization temperature (T_c is about 95°C) for the sample annealed under the pressure of 100 MPa at 75°C is less than that of the initial amorphous sample (T_c is about 101°C), it indicates that the high pressure annealing makes the crystallization temperature of PLLA reduced. For the sample annealed under 100 MPa at 85°C for 6 h, the weak exothermic peak is observed at around 95°C, suggesting the crystallization of PLLA is not complete under the conditions. In contrast, the exothermic peak around 95°C disappears for the samples annealed at 95–145°C for 6 h, showing that the crystallization of PLLA is very sufficient. In addition, the small exothermic peak around 156°C just before the melting peak is observed for samples annealed at 85–95°C for 6 h, which is attributed to the crystalline transition from the α' to α forms, as reported previously.^{9–12} These results imply that the α' form could be formed for the samples annealed under 100 MPa at 85–95°C, as further confirmed later using WAXD data.

On the other hand, the samples annealed under 200 MPa at 105–110°C for 6 h also show endothermic and exothermic behavior which is similar to the initial amorphous sample, and it suggests that no crystallization occurs after the samples are annealed. The crystallization temperature T_c of the samples annealed under 200 MPa at 105°C and 110°C are 98°C and 93°C, respectively, and less than that of initial amorphous sample (about 101°C). These results imply that the crystallization temperature of PLLA decreases with the annealing temperature increasing under the pressure. The reason for the phenomenon is not known, anyway, one explanation could be the synergic effect attributed by pressure and temperature. In addition, only

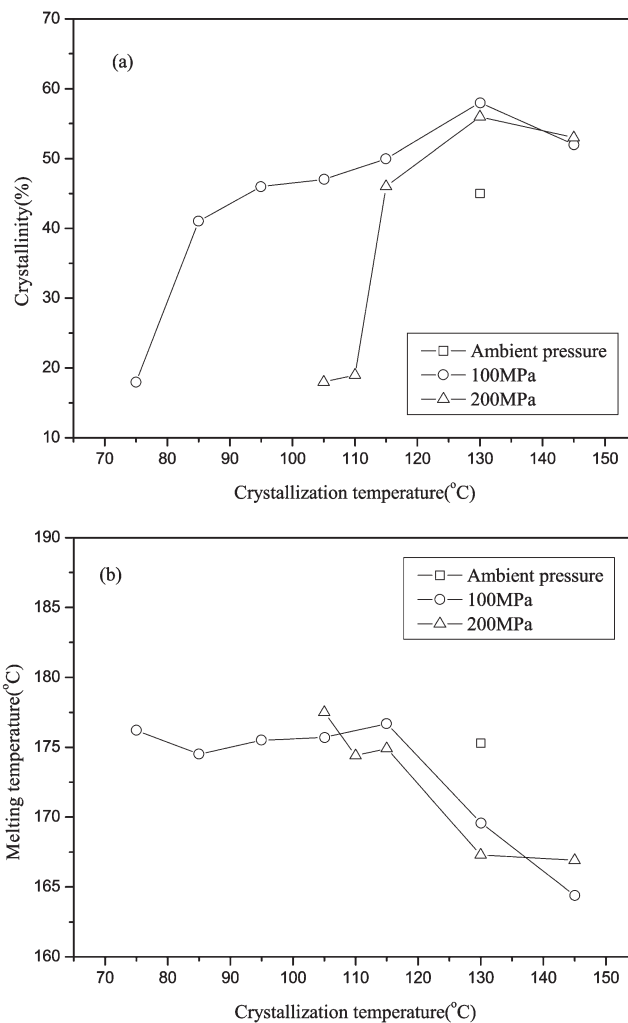


Figure 2. (a) Degree of crystallinity and (b) melting temperature for the samples annealed under ambient pressure, 100 and 200 MPa at different temperature for 6 h.

the endothermic peak around 175°C is observed for the samples annealed under 200 MPa at 115–145°C for 6 h, implying that the crystallization of PLLA is complete by annealing at the conditions. Peculiarly, no exothermic peak prior to the melting peak can be found on the DSC curves of all PLLA samples annealed under 200 MPa, which is very different from the results under 100 MPa. It means that no α' form is formed under the temperature–pressure condition. Furthermore, the sample annealed under ambient pressure at 130°C for 6 h exhibits a single melting peak, suggesting the formation of normal α crystals, similar to Zhang’s report.¹²

The degree of crystallinity (x_{c_DSC}) and the melting points (T_m) of the samples annealed under different pressure–temperature conditions determined from DSC curves are shown in Figure 2(a,b). The annealed PLLA shows the double melting behavior according to the curves of DSC, the high T_m is chose for compare. As shown in Figure 2(a), the x_{c_DSC} of the samples annealed under 100 MPa and 200 MPa increases with increasing temperature. The samples annealed under high pressure show a maximum value of x_{c_DSC} at 130°C, suggesting that the annealing temperature $T_a = 130^\circ\text{C}$ is

probably the suitable temperature for crystallinity of amorphous PLLA under 100 and 200 MPa. In addition, a dramatic increase in x_{c_DSC} is observed at the range of 75–85°C and 110–115°C for the samples annealed under 100 and 200 MPa respectively, which imply the crystalline temperature for the two samples are around 85°C and 115°C. Obviously, the pressure elevates the crystalline temperature. It can be explained by the increase of under-cooling ($\Delta T = T_m - T_c$) with pressure.¹⁷ From Figure 2(b), the T_m of the samples annealed under 100 MPa is almost a constant at $T_a = 75$ –115°C, but decreases with increasing temperature at $T_a = 115$ –145°C. As represented by the Thomson-Gibbs equation, T_m increases with increasing lamellar thickness.²⁰ Based on it, we speculate that lamellar thickness of PLLA annealed under 100 MPa become thinner at above $T_a = 115$ °C. The similar results are also observed within the samples annealed under 200 MPa at $T_a = 105$ –145°C. The DSC results may indicate that the two different crystallization mechanisms occur during the annealing process at high and low temperature under high pressure. In addition, it is found that the x_{c_DSC} of samples annealed under pressure is higher than that under ambient pressure, but the T_m of the former is lower than the latter. These results can be attributed to the mobility of chain segment confined by high pressure. Kovarski had reported that the free volume of sample increases as temperature is increased however an increase in pressure decreases the free volume.²¹ Therefore, the temperature could improve the mobility of molecular chains, leading to the increase of crystallinity. In addition, the pressure could restrict the diffusion of molecular chains, and lead to the decrease of lamellar thickness.

WAXD Measurements

Figure 3 shows WAXD profiles of the PLLA samples annealed under various temperature–pressure conditions for 6 h. As shown in Figure 3, an amorphous halo is observed for the sample annealed under 100 MPa at 75°C, and the crystallinity of the sample (about 18% as shown in Table I) is slightly larger than that of the initial sample (about 16%), which suggest that no crystallization occurs in the annealing process. However, two obvious sharp diffraction peaks are observed at $2\theta = 16.5$ and 18.9° for the samples annealed under 100 MPa at 85–95°C, while $2\theta = 16.7$ and 19.1° for the ones annealed at 115–145°C. It has been reported that the diffraction peaks at $2\theta = 16.7$ and 19.1° are observed only in the α form, whereas the diffraction peaks $2\theta = 16.5$ and 18.9° appear only in the α' form.^{6,7,9–12} In addition, a relatively small diffraction peak $2\theta = 24.5^\circ$ according to the α' form,^{9–12} is observed for the PLLA samples annealed under 100 MPa at 85–95°C. A relatively weak diffraction peak at $2\theta = 22.4^\circ$ according to the α form,^{6,7,9–12} also presents for annealed at 115–145°C. From above, we can conclude that the crystal formed at 85–95°C is α' -crystal, and the one formed at 115–145°C is α -crystal during annealing under 100 MPa for 6 h. For the sample annealed under 100 MPa at 105°C; however, four diffraction peaks appear at $2\theta = 16.6^\circ$, 19.0° , 22.4° , and 24.5° , respectively. It means that the sample annealed under 100 MPa at 105°C is a mixture, in which α' and α crystal coexist.

On the other hand, an amorphous halo is observed for the PLLA samples annealed under 200 MPa at 105–110°C, implying no crystallization occurring in the annealing process. For the

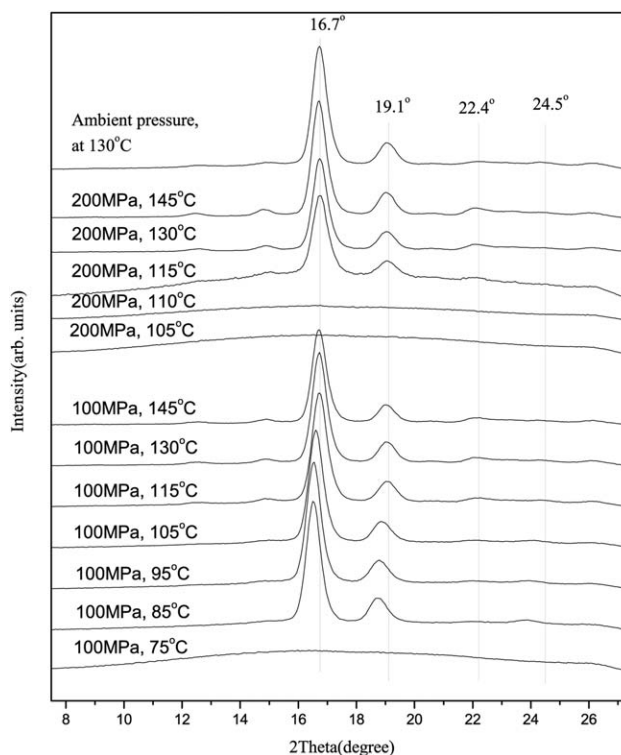


Figure 3. WAXD profiles of PLLA samples annealed under 100 and 200 MPa at different temperature and under ambient pressure at 130°C for 6 h.

samples annealed under 200 MPa at 115–145°C, strong diffraction peaks are located at $2\theta = 16.7$ and 19.1° , and a relatively weak diffraction peak at $2\theta = 22.4^\circ$ were observed. It suggests that only α form is formed during annealing under 200 MPa at 115–145°C. We speculate that α form may transform directly from the amorphous phase rather than α' form, different from the results under 100 MPa.

Combining the DSC and WAXD results, it has been found that crystal modifications of PLLA are related to not only temperature but also pressure. A phase diagram of crystalline structure of the annealed PLLA under high pressure is presented in Figure 4 according the experimental results. It needs stating that the crystalline temperature $T_c = 80^\circ\text{C}$ and transition temperature $T_{\alpha'-\alpha} = 100^\circ\text{C}$ of PLLA at ambient pressure originate from the literature.¹² From Figure 4, it can be seen that both T_c and $T_{\alpha'-\alpha}$ increase with increasing pressure. Furthermore, the temperature difference ($\Delta T = T_{\alpha'-\alpha} - T_c$) become small gradually with increasing pressure, so the α' -crystal can be formed under different temperature and pressure condition (as shown in the dash area of Figure 4). Since the α' -crystal is not observed during the heating under 200 MPa at 115–145°C for 6 h, we deduce that there may exist a critical point C (as shown in Figure 4) on the P - T_c curve at below 200 MPa. At point C, PLLA may be glass, α' and α form, or a mixture of ones or twos.

The results presented above show clearly that the α' form can be formed during the annealing within the limited temperature–pressure range. It can be explained by the shrunken free

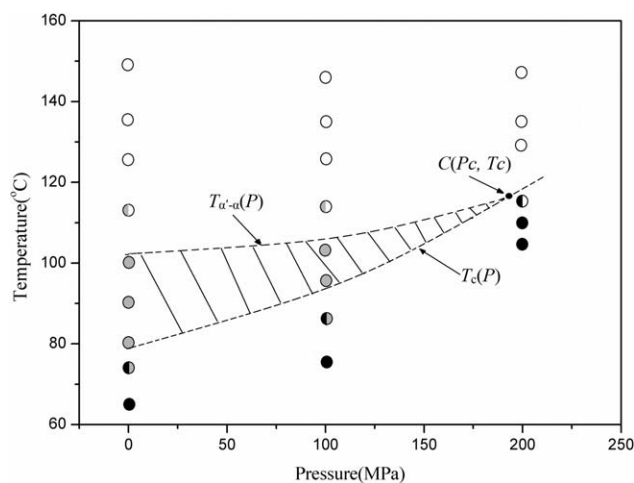


Figure 4. Phase diagram of crystalline structure of the annealed PLLA under different pressure-temperature conditions. Black, gray, and white circles represent the amorphous phase, α' -crystal and α -crystal, respectively.

volume and the confined crystallization behavior under high pressure. Under high pressure, the decrease of the free volume as well as the increase of inter-molecular interaction induced by pressure restricts chain movement of PLLA in the limited space, so the phase transition temperature increases with the increase of pressure. However, the compression rate of amorphous phase is higher than that of the α' crystal, so the increase of T_c is faster than that of $T_{\alpha'-\alpha}$ with the increase of pressure. Consequently, there exists an intersection of the P - T_c and the P - $T_{\alpha'-\alpha}$ at which the temperature and pressure is T_c and P_c , respectively. It suggests that the α' crystal can form below P_c and can not above P_c by the high pressure annealing.

SEM Measurements

To study the morphology of PLLA, SEM micrographs of fracture surfaces of PLLA annealed under 100 MPa at 95, 115, 130°C and under ambient pressure at 130°C for 6 h are illustrated in Figure 5. A great difference between the PLLA annealed under ambient pressure and 100 MPa is shown in Figure 5(a-d), respectively. The fracture surface of PLLA annealed under ambient pressure shows a compact microstructure that is comprised of many spherulites, as shown in Figure 5(a). By contrast, the fracture surface of PLLA annealed under 100 MPa at 95°C is covered by fibrillar crystalites with many sheaflike structure, as same as α' -form formed under ambient pressure.²² The PLLA annealed under 100 MPa at 115°C reveals an orderly lamellar crystalline structure with many thin films. Furthermore, the PLLA annealed under 100 MPa at 130°C exhibits some disordered rock layer-shaped surface with the thick lamellar crystalline array. These results suggest that the morphology of PLLA is significantly improved through the applied high-pressure treatment. It can be explained by the low growth rate and the diffusion of chain segment confined by high pressure.¹⁷

CONCLUSIONS

In summary, the crystalline structure and morphology of PLLA formed under various pressure and temperature conditions have been studied by differential scanning calorimetry (DSC), wide-angle X-ray diffraction (WAXD), and scanning electron microscopy (SEM). The DSC and WAXD results indicate that the α' crystal is formed under 100 MPa at 85–95°C and not formed under 200 MPa by the annealing method. A phase diagram of crystal form under high pressure is constructed under the given experimental conditions. By SEM measurement, it is clarified that the PLLA samples annealed under 100 MPa crystallize to

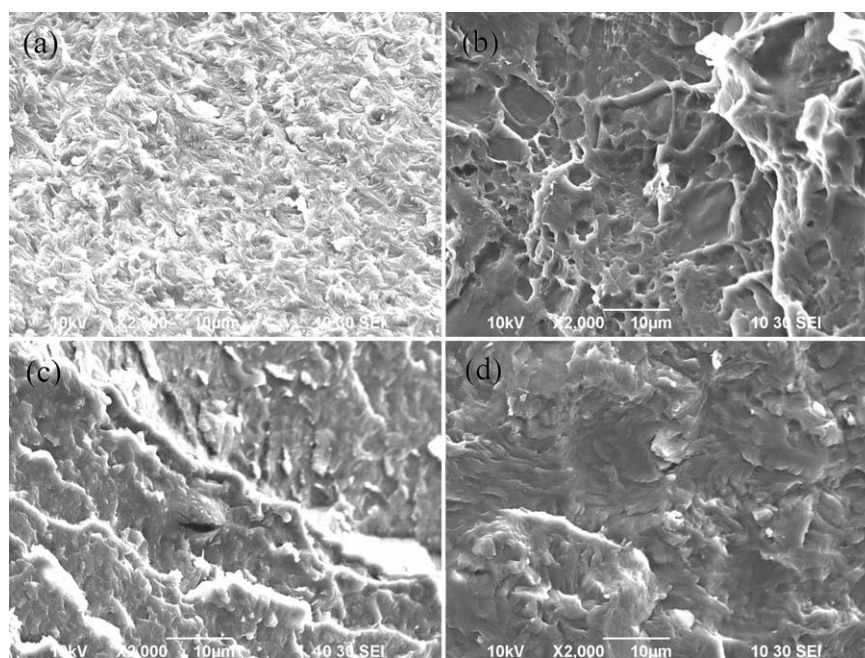


Figure 5. SEM micrographs of fracture surface of PLLA annealed (a) at 130°C under ambient pressure, and (b) at 95°C, (c) 115°C, and (d) 130°C under 100 MPa for 6 h.

form lamellar-like crystals due to the low growth rate and the confined crystallization behavior under high pressure.

ACKNOWLEDGMENTS

The authors would like to thank Lu Jun, Southwest Jiaotong University, for his useful discussion; Shao Chunguang and Dai Xin, Zhengzhou University, He Linghao, Zhengzhou University of Light Industry, for their help with experiment and characterization. The authors are grateful to the National Natural Science Foundation of China (Grant Nos. 21273206, 51002144 and 31201377) for financial support.

REFERENCES

1. Nijenhuis, A. J.; Grijpma, D. W.; Pennings, A. J. *Macromolecules* **1992**, *25*, 6419.
2. Thomson, R. C.; Wake, M. C.; Yaszemski, M. J.; Mikos, A. G. *Adv. Polym. Sci.* **1995**, *122*, 245.
3. Kim, H. D.; Bae, E. H.; Kwon, I. C.; Pal, R. R.; Nam, J. D.; Lee, D. S. *Biomaterials* **2004**, *25*, 2319.
4. Darder, M.; Aranda, P.; Ruiz-Hitzky, E. *Adv. Mater.* **2007**, *19*, 10, 1309.
5. Nair, L.; Laurencin, C. T. *Prog. Polym. Sci.* **2007**, *32*, 762.
6. Santis, P. D.; Kovacs, A. J. *Biopolymers* **1968**, *6*, 299.
7. Hoogsteen, W.; Postema, A. R.; Pennings, A. J.; ten Brinke, G.; Zugenmaier, P. *Macromolecules* **1990**, *23*, 634.
8. Cartier, L.; Okihara, T.; Ikada, Y.; Tsuji, H.; Puiggali, J.; Lotz, B. *Polymer* **2000**, *41*, 8909.
9. Kawai, T.; Rahman, N.; Matsuba, G.; Nishida, K.; Kanaya, T.; Nakano, M.; Okamoto, H.; Kawada, J.; Usuki, A.; Honma, N.; Nakajima, K.; Matsuda, M. *Macromolecules* **2007**, *40*, 9463.
10. Pan, P.; Kai, W.; Zhu, B.; Dong, T.; Inoue, Y. *Macromolecules* **2007**, *40*, 6898.
11. Pan, P.; Zhu, B.; Kai, W.; Dong, T.; Inoue, Y. *J. Appl. Polym. Sci.* **2008**, *107*, 54.
12. Zhang, J. M.; Tashiro, K. J.; Tsuji, H.; Domb, A. J. *Macromolecules* **2008**, *41*, 1352.
13. Pan, P. J.; Zhu, B.; Kai, W. H.; Dong, T.; Inoue, Y. *Macromolecules* **2008**, *41*, 4296.
14. Di Lorenzo, M. L.; Cocca, M.; Malinconico, M. *Thermochim. Acta* **2011**, *522*, 110.
15. Ahmed, J.; Varshney, S. K.; Zhang, J. X.; Ramaswamy, H. S. *J. Food Eng.* **2009**, *93*, 308.
16. Marubayashi, H.; Akaishi, S.; Akasaka, S.; Asai, S.; Sumita, M. *Macromolecules* **2008**, *41*, 9192.
17. Huang, S. Y.; Li, H. F.; Yu, D. H.; Jiang, S. C.; Chen, X. S.; An, L. J. *CrystEngComm* **2013**, *15*, 4372.
18. Xi, D. K.; Zhang, D. P.; Tian, J. J.; Lu, J.; Zhou, Z. W.; Yuan, C. S.; Liu, X. R.; Long, S. R.; Huang, Y. J.; Huang, R. *J. Macromol. Sci. Part B: Phys.* **2012**, *51*, 510.
19. Hoffman, J. D.; Weeks, J. J. *J. Res. Natl. Bur. Stand. (US)* **1962**, *66A*, 13.
20. Keith, H. D. In *Physics and Chemistry of the Organic Solid State*; Fox, D., Labes, M. M., Weissberger, A., Eds., Vol. 1, p 462. Interscience Publisher: New York, **1963**.
21. Kovarski, A. L. *High Pressure Chemistry and Physics of Polymers*; CRC Press Inc.: Boca Raton, FL, **1994**.
22. Zhang, J. M.; Duan, Y. X.; Sato, H.; Tsuji, H.; Noda, I.; Yan, S.; Ozaki, Y. *Macromolecules* **2005**, *38*, 8012.